Reactions of photogenerated fluorine atoms with contaminant molecules trapped in solid argon

5.* EPR spectroscopy of $FC_{60}^{\bullet}$ radical in solid argon

E. Ya. Misochko,[a]★ A. V. Akimov,[a] V. A. Belov,[a] and D. A. Tyurin[b]

[a]*Institute of Problems of Chemical Physics, Russian Academy of Sciences, 1 prosp. Akad. Semenova, 142432 Chernogolovka, Moscow Region, Russian Federation. E-mail: misochko@icp.ac.ru*

[b]*Department of Chemistry, M. V. Lomonosov Moscow State University, 1 Leninskie Gory, 119992 Moscow, Russian Federation*

Reactions of photogenerated fluorine atoms with C_{60} fullerene molecules isolated in solid argon were studied by EPR spectroscopy in the temperature range from 15 to 25 K. Highly resolved anisotropic EPR spectrum of the $FC_{60}^{\bullet}$ radical was obtained for the first time. The spectrum is characterized by low anisotropy of the *g*-tensor and by axially symmetric HFC tensor on ^{19}F nuclei. The parameters of the HFC tensor for ^{19}F magnetic nuclei were determined. The isotropic HFC constant A_{iso} equals 202.8 MHz and the anisotropic magnetic dipole-dipole interaction constant A_{dip} equals 51.8 MHz. Quantum chemical calculations of $FC_{60}^{\bullet}$ radical showed that the PBE1/Λ22m method (PBE1 functional and the correlation triple-zeta basis sets augmented with polarization functions on inner atomic shells) provides good agreement between the theoretical magnetic parameters and experimental data. Specific features of the spin density distribution in the $FC_{60}^{\bullet}$ radical are discussed.

Key words: cryochemistry, EPR spectroscopy, fluorine, fullerenes, radicals.

High mobility of fluorine atoms in solid argon provides a unique possibility of carrying out atom-molecule reactions involving these atoms and molecules isolated in the solid matrix. Owing to migration in the crystal an atom approaches the isolated molecule of the other reactant. The environment of the reaction complex serves a kind of microreactor, which acts as the heat sink and precludes spatial separation of the reaction products. Earlier,[1—5] we established the conditions for stabilization of radical products generated in some atom-molecule reactions ($F + CH_4$, $F + NH_3$, $F + C_2H_2$, $F + O_3$, F + HCN). This makes it possible to stabilize intermediates under ideal isolation conditions in the solid matrix and thus to fulfill the spectroscopic potential of the matrix isolation technique, as applied to IR Fourier and EPR experiments.

Our previous studies[1—5] were carried out with small reactants molecules, such as CH_4, NH_3, HCN, and O_3. They replace argon atoms in the matrix crystal lattice and cause almost no disturbance of the nearest environment in the crystal. Because of this a fluorine atom migrating in solid argon penetrates the first coordination sphere of the impurity molecule with ease; this provides high efficiency of the reaction. In this work we studied the possibility of reactions of fluorine atoms with large molecules (incorporation of such species into the argon crystal lattice creates large spatial defects). The size of the C_{60} fullerene molecule is about 1 nm, which is much larger than the distance between adjacent argon atoms in the crystal. The aim of this work was to study the conditions for stabilization of $FC_{60}^{\bullet}$ radicals generated in the reaction $F + C_{60}$, to measure the magnetic parameters of the radicals stabilized, and to establish the spin density distribution in the $FC_{60}^{\bullet}$ radical by comparing the experimental parameters of the HFC tensor with the results of quantum chemical calculations.

EPR spectroscopy is widely used in studies of radical derivatives of C_{60} fullerene to reveal specific features of the electronic structures and to predict the reactivities of such intermediates.[6—10] Nevertheless, the published data obtained for EPR measurements in liquids characterize only the isotropic parameters of the magnetic tensors. This is typical of measurements in liquids at ambient temperatures because fast molecular rotation averages the anisotropic components of the HFC and *g*-tensors. However, it is non-spherical p-AOs that are responsible for the unpaired electron density distribution in this type of radicals, but information on anisotropic interactions is lost when measurements are carried out in liquids. The isotropic HFC constants of this type of radicals are to a greater extent due to the spin polarization of inner s-shells and

* For Part 4, see Ref. 1.

Published in Russian in *Izvestiya Akademii Nauk. Seriya Khimicheskaya,* No. 3, pp. 424—428, March, 2007.

1066-5285/07/5603-0438 © 2007 Springer Science+Business Media, Inc.

only provide indirect information on the spin populations on atoms. Using parameters of the anisotropic hyperfine structure (HFS) of the EPR spectra of $FC_{60}^{\bullet}$ radical determined for the first time in this work, one can extract direct information on the "inner" interactions of the unpaired electron in the molecules under study. Comparison of the results of quantum chemical calculations obtained in this work with the corresponding experimental values made it possible to provide better characterization of the properties and specific features of the electronic structure of this type of radical intermediates.

Experimental

The base unit of the experimental setup and the procedure for EPR measurements were described in detail earlier.[2] Thin argon films were grown by co-condensation of an $Ar+F_2$ gaseous mixture and C_{60} molecular beam on the substrate of a helium cryostat cooled to 15 K. The molecular beams were co-deposited on the lower end of a flat sapphire rod from two spatially separated nozzles. The C_{60} molecular beam was generated by sublimation of C_{60} fulleride powder placed in a quartz ampoule heated to ~673—723 K with an external heater (home-made accessory for the helium cryostat). The design of the molecular beam condensation system is shown in Fig. 1. Preliminarily, we chose the heating regime of the fulleride-containing quartz ampoule, which provided an optimum rate of the molecular deposition of C_{60} on the sapphire rod (~10^{12} molecule min^{-1}). The fulleride film growth rate was determined from the interferogram of a He—Ne laser beam (λ = 632.8 nm) reflected from the surfaces of the growing film (see Fig. 1). The film thickness was calculated using the emission wavelength in vacuum. The molecular beam deposition rate thus determined served as the upper estimate of this parameter. Therefore, we can only estimate the upper bound of the C_{60} concentration in the samples under study, namely, $C_{60}/Ar \approx (1—2)\cdot 10^{-4}$.

Fluorine atoms were generated by photolysis of F_2 molecules with an UV laser (λ = 337 nm). Preliminary experiments showed that photolysis of C_{60}-containing argon films ($Ar/C_{60} \geq 10^4$) produces no radical species. Thermal diffusion of fluorine atoms in solid argon unfreezes at $T > 20$ K. In order to distinguish between the reactions of photogenerated "hot" and diffusing "thermalized" fluorine atoms, photolysis of F_2 molecules in the $Ar—F_2—C_{60}$ samples was performed at T = 15 K. Reactions of the thermal atoms occurred on heating. The sample were heated to 25 K and subsequently annealed at this temperature for ~40 min to initiate reactions of thermal fluorine atoms.

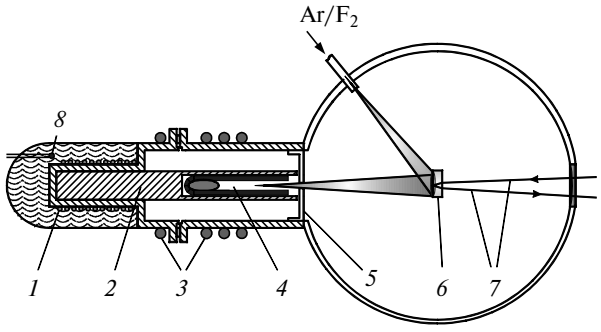

Fig. 1. Design of the cell for high-temperature sublimation of fulleride and the molecular beam condensation system: external heater helix (*1*); cylindrical copper insert (*2*); external cell housing coolant helix (*3*); quartz cell filled with fulleride powder (*4*); diaphragm separating the heated cell and the evacuated compartment of the helium cryostat (*5*); sapphire rod cooled to 15 K (*6*); He—Ne laser beam directions for control of film growth on the rod surface (*7*); and thermocouple (*8*).

Quantum chemical calculations were carried out by the density functional method using the hybrid functionals B3LYP,[11] PBE1,[12] and the generalized gradient functional PBE[13] with the correlation double- (Λ1) and triple-zeta (Λ2m) basis sets including those augmented with polarization functions on the inner atomic shells (Λ11 and Λ22m).[14] To reduce the computing time, the exchange-correlation density was expanded over an auxiliary basis set.[15] The accuracy of integration of the exchange-correlation functional was 10^{-9} a.u. In solving the electronic problem the self-consistency procedure was conducted until a gradient norm of 10^{-8} a.u. The geometric parameters of the calculated structures were optimized until a gradient norm of 10^{-5} a.u. All calculations were carried out using the PRIRODA-04 program package.[16]

Results and Discussion

Photolysis of samples at 15 K. The EPR spectra of the samples studied usually show the presence of some amount of $^{\bullet}CH_3$ radicals that are detected at maximum sensitivity of the data acquisition system (Fig. 2, curve *1*). The EPR spectrum of methyl radicals in solid argon films was observed upon heating of the quartz ampoule located at a 5-cm distance from the sapphire rod to ~400—500 °C (even if the ampoule was empty). The appearance of trace amounts of $^{\bullet}CH_3$ radicals in the EPR spectra of the

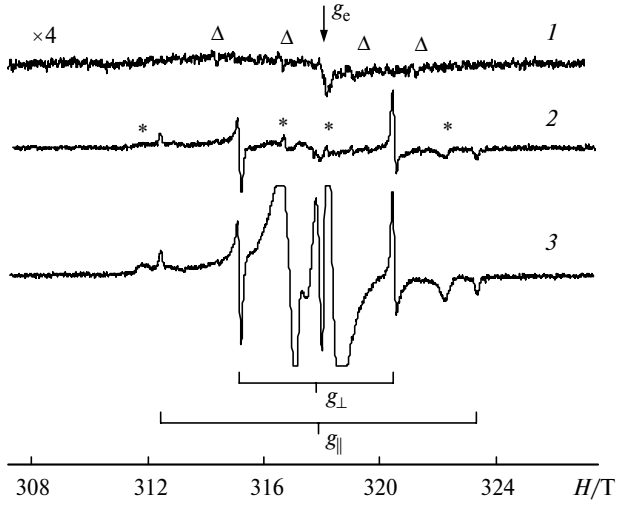

Fig. 2. EPR spectra of $Ar—C_{60}—F_2$ samples at 15 K: freshly prepared sample (symbol "Δ" denotes the EPR lines of $^{\bullet}CH_3$ radicals) (*1*); after F_2 photolysis at 15 K (EPR lines of $FO_2^{\bullet}$ radicals are asterisked) (*2*); and after annealing of the photolyzed sample at 25 K (*3*).

samples is likely due to the interaction between the residual vapor of the oil-vapor pump and the hot oven surface (despite the fact that the pump is separated from the evacuated compartment of the cryostat by the nitrogen trap). When analyzing the results of measurements, we used the EPR spectrum of $^{\bullet}CH_3$ radical ($g(^{\bullet}CH_3) = 2.0024$ in solid argon) as the reference spectrum for the determination of the *g*-factor of the species under study.

Photolysis of the $Ar—F_2—C_{60}$ samples gives rise to EPR spectra two of different radical species. Initially, the spectral line intensities increase in proportion to the duration of photolysis. In the case of prolonged photolysis (light intensity is 10 mW cm^{-2}) the EPR signal increases at a lower rate and the line intensities reach their limiting values after about 60 min. The duration of the photolytic reactions corresponds to complete consumption of F_2 molecules in the sample.[2]

The EPR spectrum of the sample recorded after switching the laser off is shown in Fig. 2 (curve *2*). The lines in the central portion of the spectrum (asterisked) can be attributed to $FO_2^{\bullet}$ radical. Molecular oxygen is the major impurity in gaseous fluorine used in the experiments; it is always present in the samples under study in a molar concentration of about 10^{-5}. Therefore, the EPR spectra of $FO_2^{\bullet}$ radical always appear upon photogeneration of F atoms and their thermal reactions at $T > 20$ K. The EPR spectrum of the second radical species has much more intense lines and corresponds to random orientation of particles with a doublet splitting in the HFS and axially symmetric HFC tensor. The linewidths in the HFS of this radical are at most 0.1 mT. Therefore, the corresponding resonance magnetic fields were determined with an accuracy of no worse than ±0.03 mT. The EPR spectrum of the second radical appears only in the samples containing both C_{60} and F_2 molecules. Therefore, it was attributed to the $FC_{60}^{\bullet}$ radical with the doublet splitting on the magnetic ^{19}F nucleus. The parameters of the anisotropic HFC tensor determined from the EPR spectrum are as follows: $A_{\parallel} = 10.90$ mT and $A_{\perp} = 5.36$ mT. The *g*-tensor anisotropy is low ($g_{\parallel} = 2.0023$, $g_{\perp} = 2.0030$, $\Delta g = |g_{\parallel} - g_{\perp}| = 0.0006$), being comparable with the linewidths, and approaches the spectral resolution value. The isotropic component of the HFC tensor is

$$A_{iso} = (A_{\parallel} + 2A_{\perp})/3 = 7.21 \text{ mT (202.8 MHz)}$$

being in good agreement with the isotropic HFC constant of the $FC_{60}^{\bullet}$ radical measured in solution.[17] This substantiates the assignment of the spectrum to the $FC_{60}^{\bullet}$ radical. The anisotropic component of the HFC tensor (magnetic dipole-dipole interaction constant) determined for the first time is

$$A_{dip} = (A_{\parallel} - A_{\perp})/3 = 1.85 \text{ mT (51.8 MHz)}.$$

Reactions of thermal fluorine atoms at $T > 20$ K. The EPR spectrum of the photolyzed sample recorded after thermal annealing is shown in Fig. 2 (curve *3*). Diffusion of fluorine atoms in solid argon causes a significant (about 100-fold) increase in the concentration of $FO_2^{\bullet}$ radicals, which is typical of this type of experiments.[1—3] The intensity of the EPR spectrum of the $FC_{60}^{\bullet}$ radical only increases by 2—3 times. In our previous studies of the reactions of small molecules (*e.g.*, NH_3 C_2H_2, HCN) the concentrations of the radical products of the interaction between the thermal fluorine atoms with these molecules were much higher than the concentration of $FO_2^{\bullet}$ radicals. Only the reaction $F + CH_4$ also occurred with low efficiency.[2] This was explained by the barrier to the reaction in solid argon (1.7 kcal mol^{-1}), which is similar to the barrier to the gas-phase reaction $F + CH_4 \rightarrow CH_3 + HF$ (1.4 kcal mol^{-1}). The low efficiency of the $F + C_{60}$ reaction can be due to significant argon lattice distortion near the fullerene molecule, which creates an additional barrier to penetration of the fluorine atom into the region of its interaction with the double bond of the C_{60} molecule. In the EPR spectrum of the products of the reactions of photogenerated translationally "hot" atoms the subspectrum of $FC_{60}^{\bullet}$ radicals is much more intense compared to that of $FO_2^{\bullet}$ radicals (see Fig. 2, curve *2*). Owing to high spectral resolution the HFS components of the EPR spectrum of the radical can be reliably identified.

Magnetic parameters and electronic structure of $FC_{60}^{\bullet}$ radical. According to published data, fluorine atoms add to the double bonds of the C_{60} molecule. Based on this, the molecular structure of $FC_{60}^{\bullet}$ radical is ascribed a C_s point symmetry group (*i.e.*, there is a symmetry plane passing through the $C_\beta—F$ and $C_\beta—C_\alpha$ bonds).[17] This structural type implies asymmetric interactions in the plane normal to the $C_\beta—F$ bond. However, the experimental EPR spectrum of the radical corresponds to axially symmetric HFC tensor on the ^{19}F nuclei. From the spectral component widths it follows that the difference between the HFC constants in the plane normal to the $C_\beta—F$ bond, $|A_{xx} - A_{yy}|$, is less than 0.03 mT. This undoubtedly indicates high symmetry of the magnetic interactions in the C—F bond region and points to significant spin density delocalization over the fullerene surface. The magnetic parameters determined in this work are compared with the results of quantum chemical calculations and measurements in solutions in Table 1.

Because the computational potential of the B3LYP functional is well known, we focussed on analysis of the results of quantum chemical calculations carried out using the poorly studied PBE1 functional. The data in Table 1 show that calculations with the gradient-generalized functional PBE significantly underestimate the isotropic HFC constant compared to the calculations with the hybrid functionals PBE1 and B3LYP in the same basis sets. For all the functionals we have used

Table 1. Theoretical and experimental magnetic parameters of the HFS of ^{19}F atom in $FC_{60}^{\bullet}$ radical

Method of investigation	A_{iso}	A_{dip}
	mT	
PBE/Λ1//PBE/Λ1	5.036	2.061
PBE/Λ11//PBE/Λ11	4.862	2.106
PBE/Λ2m//PBE/Λ2m	5.297	2.113
PBE/Λ22m//PBE/Λ22m	5.758	2.127
PBE1/Λ1//PBE1/Λ1	5.885	2.151
PBE1/Λ11//PBE1/Λ11	5.728	2.183
PBE1/Λ2m//PBE1/Λ2m	6.214	2.156
PBE1/Λ22m//PBE1/Λ22m	6.703	2.163
B3LYP/Λ1//B3LYP /Λ1	5.854	2.119
B3LYP/Λ11//B3LYP /Λ11	5.696	2.155
B3LYP/Λ2m//B3LYP /Λ2m	6.217	2.169
B3LYP/Λ22m//B3LYP /Λ22m	6.786	2.174
EPR*	7.30 (g_{iso} = 2.0023)	—
EPR**	7.21 (g_{iso} = 2.0027)	1.85

* Data taken from Ref. 17 (*tert*-butylbenzene, 325 K, measured in liquid solution).
** This work (solid argon, 15 K).

augmentation of the double-zeta basis sets with polarization functions on the inner atomic shells does not improve the description of the isotropic HFC constant. On the contrary, the isotropic HFC constants calculated with the triple-zeta basis sets are much better described. The anisotropic component of the HFC tensor relatively weakly depends on the basis set; however, the theoretical constant A_{dip} is systematically overestimated compared to the experimental value (see Table 1). The best agreement was achieved in the B3LYP/Λ22m//B3LYP/Λ22m and PBE1/Λ22m//PBE1/Λ22m calculations. The results of these calculations are in good agreement with the experimental values and confirm a nearly axial symmetry of the HFC on the ^{19}F nucleus (calculated components of the anisotropic HFC tensor are a_{xx} = −2.182 mT, a_{yy} = −2.144 mT, and a_{zz} = 4.326 mT). Our calculations underestimate the isotropic HFC constant only by 5—7% and overestimate the anisotropic HFC constants by 12—13%. The agreement between the theoretical and experimental parameters demonstrates a rather high accuracy of the B3LYP/Λ22m//B3LYP/Λ22m and PBE1/Λ22m//PBE1/Λ22m quantum chemical calculations.

The PBE1 calculated anisotropic HFC constants (magnetic dipole-dipole interaction constants A_{dip}) of ^{13}C atoms of the fullerene surface are presented in Fig. 3. Based on these values, one can evaluate the spin populations, $\rho = A_{dip}/B_0$, of the outer p-orbitals on different atoms using the atomic anisotropic HFC constant for the ^{13}C atom (B_0 = 107.4 MHz or 3.834 mT).[18] The estimate for the C_α atom (atom C(1′)) is only 34.2%. The spin density on the outer p-orbital of the fluorine atom is also

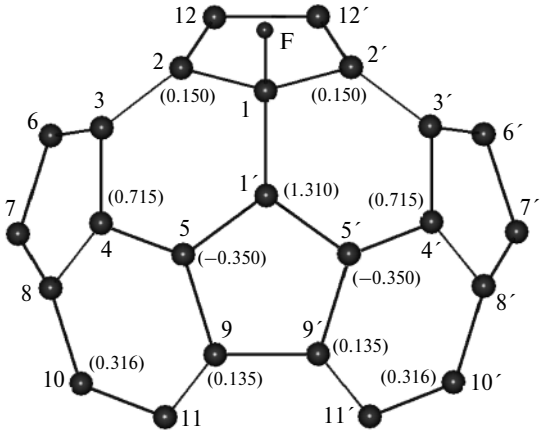

Fig. 3. Fragment of the surface of $FC_{60}^{\bullet}$ radical. Figures in parentheses denote the magnetic dipole-dipole interaction constants A_{dip} (in mT) for ^{13}C atoms obtained from PBE1/Λ22m//PBE1/Λ22m calculations.

relatively high 3.5% (atomic anisotropic HFC constant B_0 for ^{19}F equals 1760 MHz). Calculations of the Hirshfeld atomic spin populations[19] (total spin population on the electron orbitals of the corresponding atom) led to similar results, namely, 30% for the C_α atom and 3.5% for the F atom (Table 2). A large fraction of the unpaired electron spin density is also localized on the C(4) and C(4′) atoms (15.9% per atom) and on the C(10) and C(10′) atoms (6.9% per atom). The positive spin populations on these atoms induce negative spin populations on the adjacent atoms C(5) and C(5′), C(8) and C(8′), and C(11) and C(11′). About 60% of the unpaired electron spin density is localized on these carbon atoms. The re-

Table 2. Spin populations and atomic charges obtained from PBE1/Λ22m//PBE1/Λ22m calculations of $FC_{60}^{\bullet}$ radical

Atom*	$\rho^{**} = A_{dip}/B_0$	Hirshfeld spin population	Charge
$C_\beta(1)$	—	0.029	0.0974
$C_\alpha(1')$	0.341	0.300	0.0069
C(2), C(2′)	0.040	0.042	−0.0025
C(3), C(3′)	—	−0.005	−0.0022
C(4), C(4′)	0.186	0.159	0.0081
C(5), C(5′)	—	−0.042	−0.0038
C(6), C(6′)	—	0.021	−0.0003
C(7), C(7′)	—	0.025	0.0043
C(8), C(8′)	—	−0.020	−0.0014
C(9), C(9′)	0.035	0.028	−0.0014
C(10), C(10′)	0.081	0.069	0.0006
C(11), C(11′)	—	−0.014	0.0013
C(12), C(12′)	—	0.005	0.0068
F	0.035	0.035	−0.1319

* The numbering scheme of carbon atoms is given in Fig. 3.
** p-AO spin population.

maining spin density (40%) is distributed over other carbon atoms of the C_{60} fullerene surface in different fashion. Thus, the results of our calculations show an asymmetric spin density distribution. Nevertheless, the HFC tensors for the key carbon atoms C(1′), C(2), C(2′), C(4), C(4′), C(5), C(5′), C(10), and C(10′) and for the fluorine atom are axially symmetric. The spin density is mainly localized on the outer p-orbitals of these atoms, which are oriented normal to the outer surface of the fullerene cage. Table 2 shows that the magnetic dipole-dipole interaction constants (A_{dip}) give reasonable estimates of the corresponding atomic spin populations.

The theoretical atomic charge distribution is also shown in Table 2. Calculations predict a high polarization of the C_β—F bond, other atoms on the fullerene surface being almost neutral.

The results of our experiments showed that the approach employed in this work allows fluorine-containing radical derivatives of C_{60} fullerene to be generated in solid argon. Highly resolved anisotropic EPR spectra of isolated $FC_{60}^{\bullet}$ radical were recorded for the first time. The HFC constants A_{iso} and A_{dip} determined from the EPR spectra were used as test parameters for evaluation of the possibility of using quantum chemistry methods for determination of the molecular and electronic structures of this type of molecular systems. We first obtained reasonable agreement between the experimental and theoretical HFS parameters in the EPR spectrum and determined the spin density distribution with allowance for the results of our calculations. This methodology will be used in further studies of paramagnetic fullerene derivatives, in particular, for separation and characterization of regioisomers of the $FC_{70}^{\bullet}$ radical and various *endo*-metallofullerenes.

This work was financially supported by the Russian Foundation for Basic Research (Project No. 04-03-32599) and by the Chemistry and Materials Science Division of the Russian Academy of Sciences (in the framework of the Basic Research Program No. 1).

References

1. E. Ya. Misochko, I. U. Gol´dshleger, A. V. Akimov, and C. A. Wight, *Izv. Akad. Nauk. Ser. Khim.*, 2001, 947 [*Russ. Chem. Bull., Int. Ed.*, 2001, **50**, 951].
2. E. Ya. Misochko, V. A. Benderskii, I. U. Gol´dshleger, A. V. Akimov, A. V. Benderskii, and C. A. Wight, *Izv. Akad. Nauk. Ser. Khim.*, 1997, 718 [*Russ. Chem. Bull.*, 1997, **46**, 687 (Engl. Transl.)].
3. E. Ya. Misochko, I. U. Gol´dshleger, and A. V. Akimov, *Izv. Akad. Nauk. Ser. Khim.*, 2000, 832 [*Russ. Chem. Bull., Int. Ed.*, 2000, **49**, 829].
4. E. Ya. Misochko, A. V. Akimov, and C. A. Wight, *J. Phys. Chem. A*, 1999, **103**, 7972.
5. E. Ya. Misochko, A. V. Akimov, I. U. Goldschleger, and C. A. Wight, *J. Chem. Phys.*, 2002, **116**, 10307.
6. R. Borghi, L. Lunazzi, G. Placucci, P. J. Krusic, D. A. Dixon, N. Matsuzawa, and M. Ata, *J. Am. Chem. Soc.*, 1996, **118**, 7608.
7. J. R. Morton, F. Negri, and K. F. Preston, *Acc. Chem. Res.*, 1998, **31**, 63.
8. B. Mile, *Curr. Org. Chem.*, 2000, **4**, 55.
9. B. L. Tumanskii, *Izv. Akad. Nauk. Ser. Khim.*, 1996, 2396 [*Russ. Chem. Bull.*, 1996, **45**, 2267 (Engl. Transl.)].
10. B. L. Tumanskii, R. G. Gasanov, M. V. Tsikalova, A. V. Usatov, E. V. Martynova, and Yu. N. Novikov, *Izv. Akad. Nauk. Ser. Khim.*, 2004, 1968 [*Russ. Chem. Bull., Int. Ed.*, 2004, **53**, 2051].
11. A. D. Becke, *Phys. Rev. A*, 1988, **38**, 3098.
12. C. Adamo, *J. Chem. Phys.*, 1999, **110**, 6158.
13. J. P. Perdew, K. Burke, and M. Ernzerhof, *Phys. Rev. Lett.*, 1996, **77**, 3865.
14. D. N. Laikov, *Chem. Phys. Lett.*, 2005, **416**, 116.
15. D. N. Laikov, *Chem. Phys. Lett.*, 1997, **281**, 151.
16. D. N. Laikov and Yu. A. Ustynyuk, *Izv. Akad. Nauk. Ser. Khim.*, 2005, 804 [*Russ. Chem. Bull., Int. Ed.*, 2005, **54**, 820].
17. J. R. Morton, K. F. Preston, and F. Negri, *Chem. Phys. Lett.*, 1994, **221**, 59.
18. W. Weltner, Jr., *Magnetic Atoms and Molecules*, Van Nostrand Reinhold, New York, 1983, **2**, p. 447.
19. F. L. Hirshfeld, *Theor. Chim. Acta*, 1977, **44**, 129.

Received October 20, 2006;
in revised form January 29, 2007